

DYNAMICAL PROPERTY OF PERIODIC OSCILLATIONS OBSERVED IN A COUPLED NEURAL OSCILLATOR NETWORK FOR IMAGE SEGMENTATION

Tetsuya Yoshinaga and Ken'ichi Fujimoto
Faculty of Medicine, The University of Tokushima
3-18-15 Kuramoto, Tokushima, 770-8509 Japan

Keywords: Coupled oscillator, image segmentation, dynamical system, bifurcation.

Abstract: We consider image segmentation using the LEGION (Locally-Excitatory Globally-Inhibitory Oscillator Network), and investigate dynamical properties of a modified LEGION, described by noise-free or deterministic continuous ordinary differential equations. We clarify a phenomenon of image segmentation corresponds to the appearance of a synchronized periodic solution, and the ability of segmentation depends on its symmetric properties. We study bifurcations of periodic solutions by using a computational method based on the qualitative dynamical system theory.

1 INTRODUCTION

Image segmentation technique underlies perceptual processes such as identification, recognition, and separation of different objects in a natural image. Various methods of image segmentation based on statistic, filtering, and machine learning techniques were presented (Russ, 2002). A practical image segmentation technique using the LEGION (Locally-Excitatory Globally-Inhibitory Oscillator Network) has also been proposed (Wang and Terman, 1995; Terman and Wang, 1995). It can segment different areas in an image, and then the segmented areas are rapidly exhibited in time-series. Because of the high ability of LEGION, there has been a lot of research on application to medical images (Shareef et al., 1999), implementation of analog electronic circuit (Cosp et al., 2004), and so on.

The LEGION is a coupled oscillator network consisting of oscillators, each of which has an excitatory unit and an inhibitory unit, and a global inhibitor. The dynamics of LEGION is described by nonlinear ordinary differential equations with a noise term. It is known that LEGION segments different image areas temporally and spatially, based on its own dynamics. Although its fundamental dynamics has been studied (Terman and Wang, 1995), there are no investigations for detailed dynamical structure and property of oscillations observed in the coupled oscillator net-

work. Properties of the oscillations observed in LEGION are related to its fundamental ability for image segmentation, therefore analysis of the dynamical properties enable us to design the parameters of LEGION so that it achieves optimal image segmentation.

In this paper we study dynamical properties of oscillations observed in LEGION. Because the dynamics of the original LEGION (Wang and Terman, 1995) is a stochastic dynamical system with noise terms, in order to simplify our discussion, we study a noise-free LEGION, which is a deterministic dynamical system. Bifurcation analysis is useful for designing system parameter. Through the bifurcation analysis, we clarify that a phenomenon of image segmentation corresponds to the appearance of a synchronized periodic solution, and the ability of segmentation depends on its symmetric properties.

2 MODEL DESCRIPTION

The LEGION consists of a global inhibitor and oscillators which are arranged in grid; and the number of oscillators corresponds to the number of pixels in target image. We illustrate single oscillator which consists of an excitatory unit EU_i and an inhibitory unit IU_i in Fig.1 (a). The excitatory unit couples with the other excitatory units in its four-neighborhood

each other, and all excitatory units also connect to the global inhibitor. The architecture of LEGION is shown in Fig.1 (b). Figure 1 (c) illustrates the behavior of LEGION and schematic diagram of an image segmentation procedure. The dynamics of an oscillator indexed by i ($i = 1, 2, \dots, n$) is described by

$$\frac{dx_i}{dt} = 3x_i - x_i^3 + 2 - y_i + I_i + C_i \quad (1)$$

$$\frac{dy_i}{dt} = \eta [\gamma(1 + \tanh(x_i/\beta)) - y_i]. \quad (2)$$

We eliminated noise terms from the original LEGION (Wang and Terman, 1995) so that the system becomes a deterministic dynamical system. The variables x_i and y_i represent the states of the excitatory and inhibitory units, respectively. The symbol I_i denotes external stimulation to the oscillator. Its value is determined by the i -th pixel value. The symbol C_i represents the summation of the coupling strength among oscillators, which is defined by

$$C_i = \sum_{k \in N(i)} W_{ik} S(x_k, \theta_x) - W_z S(z, \theta_{zx}) \quad (3)$$

where

$$S(x, \theta) = \frac{1}{1 + \exp(-K(x - \theta))}. \quad (4)$$

Here $N(i)$ indicates the four-neighborhood of the i -th oscillator, W_{ik} denotes the coupling strength between the i -th oscillator and the other k -th oscillator in $N(i)$, and W_z denotes the coupling strength between the i -th oscillator and the global inhibitor. Using the sigmoidal function, described by Eq.(4), instead of the Heaviside function in the original LEGION, the dynamics of the global inhibitor is defined by

$$\frac{dz}{dt} = \phi \left(S \left(\sum_{k=1}^n S(x_k, \theta_{zx}), \theta_{zx} \right) - z \right) \quad (5)$$

where $\gamma, \beta, \theta_x, \theta_{zx}, \theta_{zx}, K$, and ϕ indicate parameters, which are fixed as the same values of the original

$$\begin{aligned} \gamma &= 6.0, & \beta &= 0.1, & \theta_x &= -0.5 \\ \theta_{zx} &= \theta_{zx} = 0.1, & K &= 50, & \phi &= 3.0 \end{aligned} \quad (6)$$

and η is a bifurcation parameter.

We treat binary images shown in Figs. 2–3; the indexes of the pixels are also shown in the same figures. For the binary images, the value of I_i is determined by

$$\begin{cases} I_i > 0, & \text{if the } i\text{-th pixel is white} \\ I_i < 0, & \text{if the } i\text{-th pixel is black.} \end{cases} \quad (7)$$

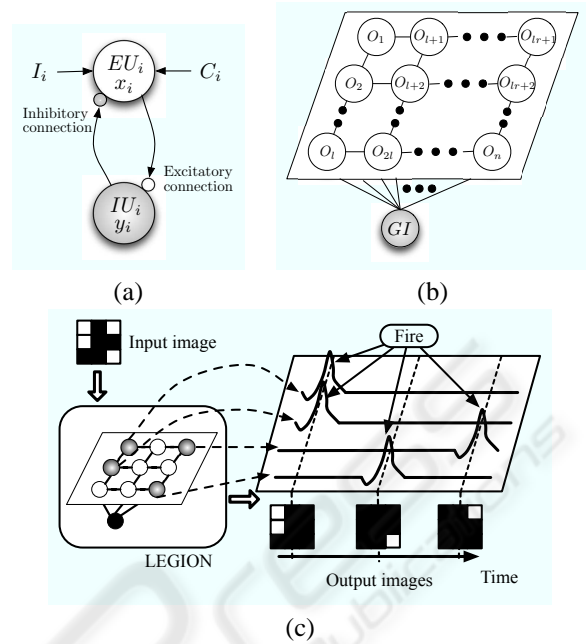


Figure 1: (a), (b) Architecture of LEGION, and (c) behavior of LEGION and schematic diagram of image segmentation.



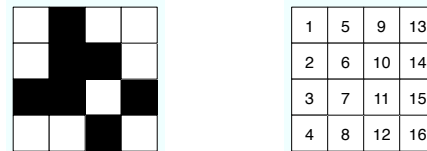
(a) Input image (b) Index number of each pixel

Figure 2: (3 × 3)-pixel image and its index number of each pixel.

3 METHOD OF ANALYSIS

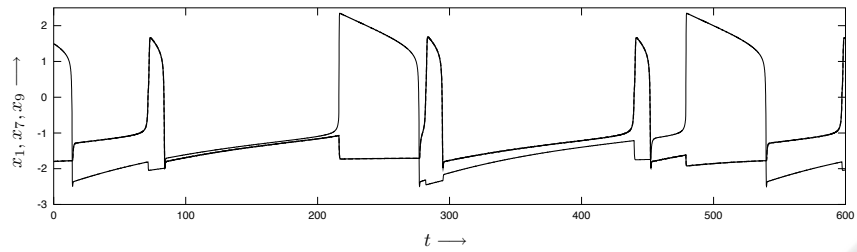
We summarize methods for calculating bifurcations in the deterministic LEGION defined in the preceding section. Let us consider an N -dimensional general autonomous differential equation consisting of Eqs.(1)–(5) such that

$$\frac{dx}{dt} = f(x). \quad (8)$$

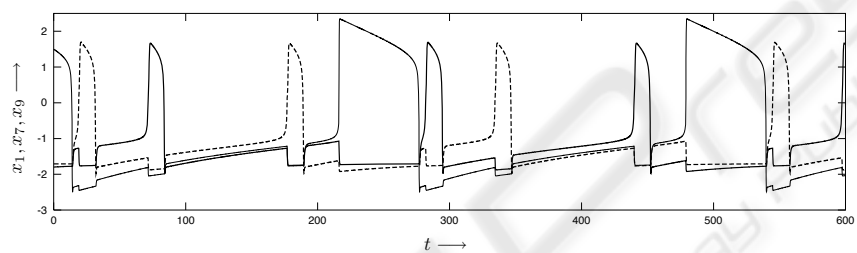


(a) Input image (b) Index number of each pixel

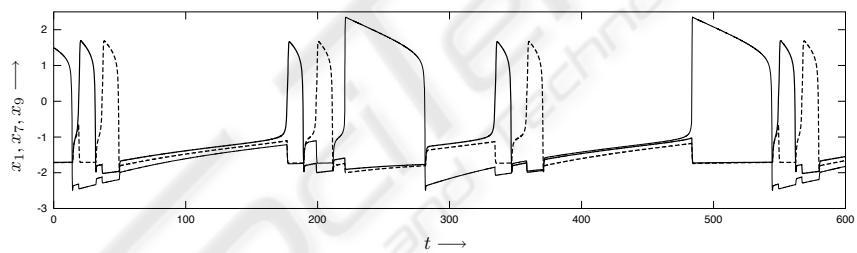
Figure 3: (4 × 4)-pixel image and its index number of each pixel.



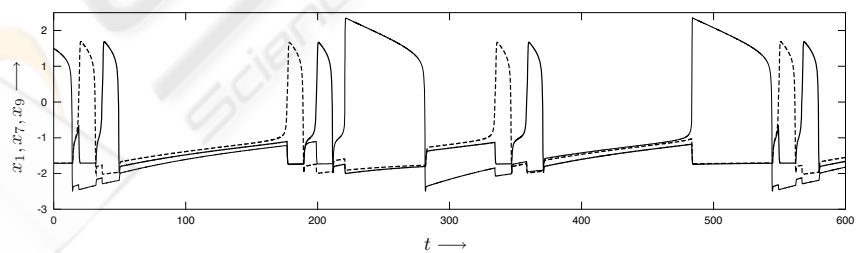
(a)



(b)



(c)



(d)

Figure 4: Waveforms of stable periodic solutions under $\eta = 0.02$. The thin solid curve indicates the states of the oscillators x_1 and x_2 ; and the heavy solid curve and the dashed curve denote the states of the oscillators x_7 and x_9 , respectively.

The state vector $x \in R^N$ corresponds to the set $\{x_1, y_1, x_2, y_2, \dots, x_n, y_n, z\} \in R^{2n+1}$, where n denotes the number of oscillators. Note that $f(x)$ is C^∞ -class function for all state variables and all parameters. We assume that there exists a solution with initial condition, $x = x_0$ at $t = t_0$, described by $x(t) = \varphi(t; x_0)$ for all t .

We consider a local manifold Σ in the N -dimension state space with the scalar condition $g(x) = 0$, which is described by

$$\Sigma = \{x \in R^N \mid g(x) = 0, g: R^N \rightarrow R\}. \quad (9)$$

We arrange a local section $\Pi \subset R^{N-1}$ in Σ called the Poincaré section. Using the coordinate transformation h described by

$$h: \Sigma \rightarrow \Pi \subset R^{N-1}; \quad x \mapsto u, \quad (10)$$

we define the Poincaré map T as

$$T: \Pi \rightarrow \Pi; \quad u \mapsto h \circ \varphi(\tau(h^{-1}(u)); h^{-1}(u)) \quad (11)$$

where $\tau(h^{-1}(u))$ is the time in which the trajectory emanating from a point $u \in \Pi$ at $t = t_0$ will go across the Π again. Then an m -periodic solution in Eq.(8) corresponds to a fixed point of T^m , i.e., m -periodic point of T . Hence, one of analyses of m -periodic solutions observed in Eq.(8) can be reduced to an analysis of a fixed point of T^m .

Let $u^* \in R^{N-1}$ be a fixed point of T^m such that

$$u^* - T^m(u^*) = 0. \quad (12)$$

Then the characteristic equation of the fixed point is defined by

$$\chi(\mu) = \det \left(\mu I_{N-1} - \frac{\partial T^m(u^*)}{\partial u} \right) = 0 \quad (13)$$

where I_{N-1} is the $(N-1) \times (N-1)$ identity matrix. By using the Poincaré map T^m we totally have $2(N-1)$ -different-type hyperbolic fixed points. The topological property of a hyperbolic fixed point is determined by the value of characteristic multipliers μ_i , ($i = 1, 2, \dots, N-1$): if all characteristic multipliers are in the unit circle on the Gaussian plane, then the fixed point is stable; the fixed point is unstable if one or more characteristic multipliers are outside the unit circle. Hence, we can discuss topological property of the fixed point based on the value of the characteristic multipliers. Let us classify fixed points into two types ${}_kD$ and ${}_kI$, where k is the number of characteristic multipliers outside the unit circle; it also represents the dimension of unstable subspace. The types D and I correspond to the even and odd numbers of characteristic multipliers in the range of $(-\infty, -1)$ on the real axis, respectively. Bifurcation of a fixed point occurs when its topological property is changed by the

variation of a system parameter. The types of bifurcations are tangent bifurcation, period-doubling bifurcation, the Neimark-Sacker bifurcation, and D -type of branching. Bifurcation sets of a fixed point are computed (Kawakami, 1984) by solving the simultaneous equation which consists of Eqs.(12)–(13).

Now, let us discuss a symmetrical property of the system in Eq.(8). Assume that there exists a transformation Q satisfying $Q(f(x)) = f(Q(x))$. Then such a system may have a periodic solution satisfying $Q(\varphi(t; x_0)) = \varphi(t + L; x_0)$ for all t , where $L \geq 0$ is a phase difference. We call it a (Q, L) -symmetric periodic solution.

4 RESULTS AND DISCUSSION

This section is devoted to show and discuss numerical results obtained from bifurcation analysis of a couple of examples.

4.1 Example 1

We investigate periodic solutions observed in the deterministic LEGION for 3×3 pixel image shown in Fig.2. Each external stimulus I_i , $i = 1, 2, \dots, 9$, is defined as

$$\begin{cases} I_i = 0.2, & \text{if the } i\text{-th pixel is white} \\ I_i = -0.02, & \text{if the } i\text{-th pixel is black.} \end{cases} \quad (14)$$

Because the pixels indexed by 1, 2, 7, and 9 are white, we observe oscillatory responses from the oscillators with the same indices, and non-oscillatory responses from the other oscillators. Note that, because the set satisfying $x_7 \equiv x_9$ and $y_7 \equiv y_9$ is an invariant subspace in the state space, the system is symmetric with respect to the transformation, say Q_1 , swapping (x_7, y_7) and (x_9, y_9) .

For oscillatory solutions we use symbolic sequence of strings representing the continuation of in-phase firing assigned by the oscillator indices and non-firing assigned by dot (“.”). For example, the set of (12.79.7.9) indicates a sequence in the order of firing: oscillators 1 and 2 (instantaneously in-phase), oscillators 7 and 9 (instantaneously in-phase), oscillator 7, and oscillator 9, periodically.

Figure 4 shows waveforms of stable periodic solutions observed in the system at $\eta = 0.02$. The symbolic sequences corresponding to Figs.4 (a)–(d) are, respectively, as follows: (a) (12.79.79.12.79); (b) (12.7.9.7.12.9.7.9); (c) (12.7.9.7.9.12.7.9); and (d) (12.9.7.9.7.12.9.7). The solutions shown in Figs.4 (a) and (b) are $(Q_1, 0)$ - and $(Q_1, \tau/2)$ -symmetric two-periodic solutions, respectively, where τ denotes the

period of solution. While, each of the solutions shown in Figs.4 (c) and (d) has no symmetric property itself, however, it is reflectional with respect to the transformation Q_1 each other. We show the time-series of output images from LEGION in Fig.5, which corresponds to the solution of Fig.4 (b). The connected white pixels, the first pixel and the second pixel, always appear instantaneously in-phase. Then three different image areas are segmented temporally and spatially.

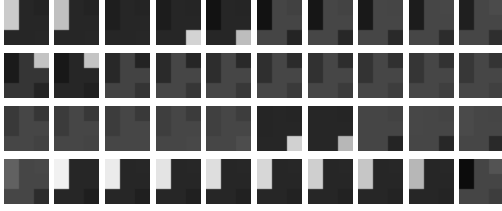


Figure 5: Snapshots of time-series output in LEGION which corresponds to the periodic solution shown in Fig. 4 (b). These output images sequentially appear from on the top-left to the bottom-right; then its appearance in each line starts from the left.

We investigate bifurcations of periodic points based on the Poincaré section defined by

$$\Pi = \left\{ x \in \mathbb{R}^N \mid x_1 - 1.5 = 0, \frac{dx_1}{dt} < 0 \right\}. \quad (15)$$

Figure 6 shows a one-parameter bifurcation diagram of a $(Q_1, 0)$ -symmetric two-periodic solution as shown in Fig.4 (a). In the bifurcation diagram, the heavy curve denotes stable $(Q_1, 0)$ -symmetric two-periodic solution, and the dashed curve indicates its destabilized solution. The circled point labeled by I^2 denotes the parameter value $\eta = 0.08098952872$, at which we observe a period-doubling bifurcation. By decreasing the value of η across the point, the following bifurcation formula occurs:

$${}_1I^2 \rightarrow {}_0D^2 + {}_1D^4 \quad (16)$$

where the left- and right-hand sides of the arrow indicate the periodic points before and after the bifurcation, respectively. Hence, a stable two-periodic solution ${}_0D^2$ and a saddle-type four-periodic solution ${}_1D^4$ simultaneously occur, i.e., they coexist in a certain parameter region. Let us discuss the basin of the stable solution. Figure 7 (a) shows periodic points of the Poincaré map at $\eta = 0.0808$, projected to the (x_7, x_9) -plane. The points a and b indicates two-periodic point ${}_0D^2$, and the points c and d correspond to a $(Q_1, \tau/2)$ -symmetric two-periodic solution, which is irrelative to the bifurcation in Eq.(16). The periodic points of the coexisting ${}_1D^4$ are near the point a . It can be confirmed by the phase portrait shown in Fig.7 (b), an enlarged figure of Fig.7 (a); the points e and f denote a

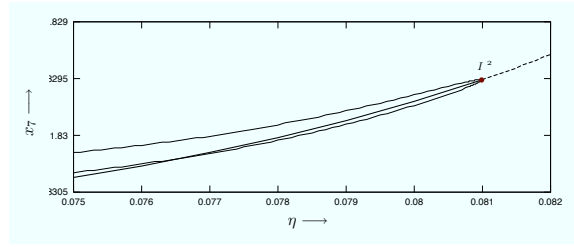


Figure 6: One-parameter bifurcation diagram of x_7 for the parameter η . The thin solid curve, the heavy solid curve, and the dashed curve denote the unstable four-periodic point, the stable two-periodic point, and its destabilized two-periodic point, respectively.

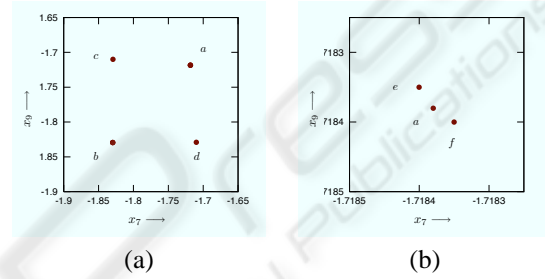


Figure 7: Phase portrait of periodic points on the (x_7, x_9) -plane under $\eta = 0.0808$. The right figure is the enlarged figure around the point a in the left figure.

part of four-periodic points ${}_1D^4$. The period-doubling bifurcation of ${}_1I^2$ occurs so that its symmetry is broken, then the placement of the periodic points are reflected in the topological property which can be explained by its eigenvector. Besides, the basin boundary of ${}_0D^2$ is separated by the stable manifold of ${}_1D^4$. That is, we can observe ${}_0D^2$ when the initial value is placed only near its periodic point.

4.2 Example 2

As the second example we treat 4×4 pixel image shown in Fig.3. The value of each external stimulus I_i , $i = 1, 2, \dots, 16$, is defined by Eq.(14); its index number i is shown in Fig.3 (b). Due to the pixels indexed by 1, 2, 4, 8, 9, 11, 13, 14, and 15 are white, the dynamical system has two symmetries for two swapping operators. One is described by $Q_2(f(x)) = f(Q_2(x))$ where Q_2 is the transformation that swaps (x_1, y_1, x_2, y_2) with (x_4, y_4, x_8, y_8) , respectively. The other symmetry is described by $Q_3(f(x)) = f(Q_3(x))$ where Q_3 is the transformation that swaps (x_{11}, y_{11}) with (x_{16}, y_{16}) . In this example, we investigate periodic solutions with the following relations: $(x_1, y_1) = (x_2, y_2)$, $(x_4, y_4) = (x_8, y_8)$, and $(x_9, y_9) = (x_{13}, y_{13}) = (x_{14}, y_{14})$. Periodic solu-

tions in Table 1 are observed under $\eta = 0.02$. Note that we employed the symbols a, b, c, \dots, g instead of the double-digit index numbers $10, 11, 12, \dots, 16$, respectively. Besides, the symbols A, B, C, D , and E represent kinds of periodic solutions. All solutions in the category A are $(Q_2, 0)$ -symmetric two-periodic solutions; the solutions A_1 and A_2 are reflectional symmetry for Q_2 , then A_3 and A_4 are also reflectional symmetry for Q_3 . The category B indicates $(Q_3, 0)$ -symmetric two-periodic solution, then B_1 and B_2 are reflectional symmetry for Q_2 . The category C denotes $(Q_3, \tau/2)$ -symmetric two-periodic solution, then C_1 and C_2 are also reflectional symmetry for Q_2 . Each periodic solution in D has two symmetries. The category D_1 is a two-periodic solution with $(Q_2, 0)$ - and $(Q_3, 0)$ -symmetric properties; the others D_2, D_3 , and D_4 are two-periodic solutions with $(Q_2, 0)$ -symmetric and $(Q_3, \tau/2)$ -symmetric. All solutions in E are asymmetric two-periodic solutions, however, respective pairs of solutions (E_1, E_2) and (E_3, E_4) are reflectional symmetry for Q_3 . The solutions (E_2, E_3) and (E_1, E_4) are also reflectional symmetry for Q_2 , respectively. Besides, in the solutions $A_3, A_4, B_3, B_4, C_3, C_4, D_1, D_4$, and E_5 , the image area connected white pixels, indexed by 9, 13, and 14, synchronously fire with the other white area, e.g., the pixels indexed by 1, 2, 4, or 8. This synchronization is interesting from a viewpoint of nonlinear science. However, it is inappropriate for image segmentation.

5 CONCLUDING REMARKS

We have investigated dynamical properties of periodic solutions observed in the deterministic LEGION, which is a modification from the original one by eliminating noise terms and replacing the Heaviside function with a sigmoidal function, in order to investigate dynamical properties and ability of LEGION. The main results obtained from the analysis using our method for computing bifurcation sets, are summarized as follows: (1) The dynamical system has various kinds of symmetric properties corresponding to the input image. Indeed we see that symmetric and asymmetric periodic solutions can be observed. Its patterns are based on the symmetric dynamical structure of LEGION; (2) A stable symmetric periodic solution bifurcates under a certain parameter. Moreover, then its basin boundary is determined by the stable manifolds of the coexisting saddle-type periodic solution; and (3) We also observed periodic solutions such that different image areas fire synchronously. The intrinsic objective of image segmentation in LEGION is that different image areas are not exhibited at the

Table 1: Periodic solutions by symbolic sequences.

Category	Periodic solutions
A_1	(1248.b.g.9de.b.g.1248.b.g.9de)
A_2	(1248.g.9de.b.1248.g.b.9de.g.b)
A_3	(12489de.g.b.g.b.12489de.g.b)
A_4	(12489de.b.g.b.g.12489de.b.g)
B_1	(12.48.bg.9de.12.bg.48.9de.bg)
B_2	(12.9de.bg.48.12.bg.9de.48.bg)
B_3	(129de.bg.48.129de.bg.48.bg)
B_4	(12.bg.489de.12.bg.489de.bg)
C_1	(12.g.9de.b.48.g.12.b.9de.g.48.b)
C_2	(12.g.48.b.9de.g.12.b.48.g.9de.b)
C_3	(129de.g.b.48.g.129de.b.g.48.b)
C_4	(12.g.b.489de.g.12.b.g.489de.b)
D_1	(12489de.bg.12489de.bg.bg)
D_2	(1248.g.9de.b.g.1248.b.9de.g.b)
D_3	(1248.b.g.9de.b.1248.g.b.9de.g)
D_4	(12489de.g.b.g.12489de.b.g.b)
E_1	(12.g.b.48.9de.g.b.12.48.g.b.9de)
E_2	(12.b.g.48.9de.b.g.12.48.b.g.9de)
E_3	(12.b.g.9de.48.b.g.12.9de.b.g.48)
E_4	(12.g.b.9de.48.g.b.12.9de.g.b.48)
E_5	(12.b.g.489de.12.b.g.489de.b.g)

same time. Therefore, the appearance of the periodic solutions is inappropriate for this objective.

Their analyzed dynamical properties are directly related to fundamental abilities of LEGION. For higher quality of the segmentation, a mechanism for desynchronizing in-phase periodic solutions is required in the coupling system.

REFERENCES

- Cosp, J., Madrenas, J., Alarcon, E., Vidal, E., and Villar, G. (2004). Synchronization of nonlinear electronic oscillators for neural computation. *IEEE Trans. Neural Networks*, 15(5):1315–1327.
- Kawakami, H. (1984). Bifurcation of periodic responses in forced dynamic nonlinear circuits: computation of bifurcation values of the system parameters. *IEEE Trans. Circuits Syst.*, CAS-31(3):246–260.
- Russ, J. (2002). *The image processing handbook, fourth Ed.* CRC Press.
- Shareef, N., Wang, D., and Yagel, R. (1999). Segmentation of medical images using legion. *IEEE Trans. Medical Imaging*, 18:74–91.
- Terman, D. and Wang, D. (1995). Global competition and local cooperation in a network of neural oscillators. *Physica*, D81:148–176.
- Wang, D. and Terman, D. (1995). Locally excitatory globally inhibitory oscillator networks. *IEEE Trans. Neural Networks*, 6(1):283–286.